Stabilization of Non-Cooperative Satellites in Low Earth Orbits using Inter-Satellite Atmospheric Drag

Espen Oland
Department of Electrical Engineering
UiT - The Arctic University of Norway
Narvik, Norway
espen.oland@uit.no

Raymond Kristiansen
Department of Electrical Engineering
UiT - The Arctic University of Norway
Narvik, Norway
raymond.kristiansen@uit.no

***Abstract*—This paper presents a novel solution to the problem of stabilization of non-cooperative satellites in low Earth orbits, which utilizes inter-satellite aerodynamic drag effects for generation of aerodynamics moments in the wake of a controlled satellite. Hence, by altering the position of a smaller controlled satellite, we are able to change the wake region and thus provide aerodynamic moments for de-spinning and attitude control of a non-cooperative satellite. The paper provides a detailed description of the problem, the proposed solution, and shows its performance through simulations. This work represents a new direction within control of non-cooperative satellites in low Earth orbits that to the authors knowledge has never been studied before.**

***Index Terms*—formation control, satellites, non-cooperative, attitude control, rate control, aerodynamic moments, wake effect**

I. Introduction

The problem of controlling non-cooperative satellites has received much attention the last decade. The general approach for controlling a non-cooperative satellite involves the use of a robotic arm or similar to grab and then stabilize the satellite -*cf.* [1], [2], [3], [4] and references therein. This paper ask the question: "*Is it possible to use the aerodynamic wake effect to generate aerodynamic moments on a non-cooperative satellite, and then use that effect to stabilize the satellite?*".

There are indeed many situations involving non-cooperative satellites where there is a need to regain control. This can be a satellite that has depleted it's thruster propellant, such that it can no longer maintain its primary mission. Then by using inter-satellite atmospheric drag, the non-cooperative satellite can be stabilized, enabling e.g. the reaction wheels to despin, thereby regaining control and prolong the lifetime of the satellite. Other situations might call for using the inter-satellite atmospheric drag to introduce translational forces to change the position of the non-cooperative satellite, thereby avoiding collisions with other satellites. A working solution will also be applicable to removal of space debris, through changing orbital elements for debris objects for a faster descent into the atmosphere.

In this paper, we present a novel solution for controlling such non-cooperative satellites in low Earth orbits, that to our knowledge has not been explored previously. The fundamental idea behind our solution is that satellites operating in orbits with a certain atmospheric density will experience some aerodynamic drag effects. When satellites with different sizes and shapes are operating close to each other, they will therefore experience differences in drag. Moreover, satellite motion will introduce similar wake effects that is seen in marine or aerial systems, albeit smaller. However, with such wake and inter-satellite drag effects present, these may be exploited for controlling a non-cooperative satellite through active operation of other satellites in its vicinity. The idea presented here share many similarities with *tugboats* used for marine applications to control large ships in berthing operations by transferring forces using direct/indirect contact to create rotational moments -*cf.* [5], [6]. To that end, the satellites creating the inter-satellite atmospheric drag are therefore named *tugsats*.

As these are preliminary results, our proposed solutions rest on some limitations. To that end, we focus on the rotational control problem, and assume that the tugsat is able to control its position perfectly relative to the non-cooperating satellite, and that generated translational forces are ignored. In addition, the problem is constrained to control in a plane relative to an inertial frame, and no orbital mechanics or leader-follower dynamics are used. Finally, CFD analyses to obtain accurate estimates in terms of the airflow hitting the non-cooperative satellite is considered outside the scope of this work. These limitations, as well as extensions to full 3D rotational control will be the topic for future work.

The paper is structured as follows: Section II describes the notation and modeling of attitude kinematics and dynamics together with details on how to model the wake effect and what its impact is on a neighboring satellite. Section III describes in detail how aerodynamic moments are calculated. In Section IV we design a rate controller that can control a non-cooperative satellite, while Section V shows through simulations the performance of the solution. In Section VI the results are discussed as well as future work needed for advancing these results further. The final conclusion is given in Section VII.

II. Modeling

A. Notation

This subsection is similar to the first author's previous works such as [7] and gives an overview of notation and

basic definitions. The time derivative of a vector is denoted as $\dot{\mathbf{x}} = d\mathbf{x}/dt$ and the Euclidean length is written as $||\mathbf{x}|| = \sqrt{\mathbf{x}^\top \mathbf{x}}$. Superscript denotes the reference frame of a vector. The rotation matrix is denoted $\mathbf{R}_a^c \in \mathcal{SO}(3) = \{\mathbf{R} \in \mathbb{R}^{3\times 3} : \mathbf{R}^\top \mathbf{R} = \mathbf{I}, \det(\mathbf{R}) = 1\}$, which rotates a vector from frame a to frame c and where $\mathbf{I}$ denotes the identity matrix.

The angular velocity vector is denoted $\boldsymbol{\omega}_{a,c}^e$, which represents the angular velocity of frame c relative to frame a referenced in frame e. Angular velocities between different frames can be added together as $\boldsymbol{\omega}_{a,f}^e = \boldsymbol{\omega}_{a,c}^e + \boldsymbol{\omega}_{c,f}^e$. The time derivative of the rotation matrix is found as $\dot{\mathbf{R}}_a^c = \mathbf{R}_a^c \mathbf{S}(\boldsymbol{\omega}_{c,a}^a)$ where the cross product operator $\mathbf{S}(\cdot)$ is such that for two arbitrary vectors $\mathbf{v}_1, \mathbf{v}_2 \in \mathbb{R}^3$, $\mathbf{S}(\mathbf{v}_1)\mathbf{v}_2 = \mathbf{v}_1 \times \mathbf{v}_2$, $\mathbf{S}(\mathbf{v}_1)\mathbf{v}_2 = -\mathbf{S}(\mathbf{v}_2)\mathbf{v}_1$, $\mathbf{S}(\mathbf{v}_1)\mathbf{v}_1 = \mathbf{0}$ and $\mathbf{v}_1^\top \mathbf{S}(\mathbf{v}_2)\mathbf{v}_1 = 0$. Given $\mathbf{v}_1 = \begin{bmatrix} v_1 & v_2 & v_3 \end{bmatrix}^\top$ the operator is defined as

$$\mathbf{S}(\mathbf{v}_1) = \begin{bmatrix} 0 & -v_3 & v_2 \\ v_3 & 0 & -v_1 \\ -v_2 & v_1 & 0 \end{bmatrix}. \tag{1}$$

The rotation matrix is parameterized using unit quaternions, where the quaternion that represents a rotation from frame a to frame c is denoted $\mathbf{q}_{c,a} \in \mathcal{S}^3 = \{\mathbf{q} \in \mathbb{R}^4 : \mathbf{q}^\top \mathbf{q} = 1\}$. We write this quaternion as $\mathbf{q}_{c,a} = \begin{bmatrix} \eta_{c,a} & \boldsymbol{\epsilon}_{c,a}^\top \end{bmatrix}^\top = \begin{bmatrix} \cos\left(\frac{\vartheta_{c,a}}{2}\right) & \mathbf{k}_{c,a}^\top \sin\left(\frac{\vartheta_{c,a}}{2}\right) \end{bmatrix}^\top$ which performs a rotation of an angle $\vartheta_{c,a}$ around the unit vector $\mathbf{k}_{c,a}$. The inverse quaternion is defined as $\mathbf{q}_{a,c} = \begin{bmatrix} \eta_{c,a} & -\boldsymbol{\epsilon}_{c,a}^\top \end{bmatrix}^\top$. The scalar part is denoted $\eta_{c,a}$ and the vector part as $\boldsymbol{\epsilon}_{c,a} \in \mathbb{R}^3$, enabling the rotation matrix to be constructed as $\mathbf{R}_a^c = \mathbf{I} + 2\eta_{c,a}\mathbf{S}(\boldsymbol{\epsilon}_{c,a}) + 2\mathbf{S}^2(\boldsymbol{\epsilon}_{c,a})$. Composite rotations are found using the quaternion product as $\mathbf{q}_{c,e} = \mathbf{q}_{c,a} \otimes \mathbf{q}_{a,e} = \mathbf{T}(\mathbf{q}_{c,a})\mathbf{q}_{a,e}$ with

$$\mathbf{T}(\mathbf{q}_{c,a}) = \begin{bmatrix} \eta_{c,a} & -\boldsymbol{\epsilon}_{c,a}^\top \\ \boldsymbol{\epsilon}_{c,a} & \eta_{c,a}\mathbf{I} + \mathbf{S}(\boldsymbol{\epsilon}_{c,a}) \end{bmatrix}, \tag{2}$$

which ensures that the resulting quaternion maintains the unit length property.

B. Attitude Kinematics and Dynamics

Let us consider two reference frames, an inertial frame denoted by i, and a body frame of the non-cooperative satellite denoted by b. The inertial reference frame is considered a right-handed fixed reference frame, while the body frame aligns with the principle axes of inertia of the non-cooperative satellite, with origin in the center of mass and moves with the satellite. Using quaternions to parameterize the attitude, the attitude kinematics and dynamics can be described as (*cf.* [8])

$$\dot{\mathbf{q}}_{i,b} = \frac{1}{2}\mathbf{q}_{i,b} \otimes \begin{bmatrix} 0 \\ \boldsymbol{\omega}_{i,b}^b \end{bmatrix} \tag{3}$$

$$\mathbf{J}\dot{\boldsymbol{\omega}}_{i,b}^b = -\mathbf{S}(\boldsymbol{\omega}_{i,b}^b)\mathbf{J}\boldsymbol{\omega}_{i,b}^b + \boldsymbol{\tau}_a^b + \boldsymbol{\tau}_p^b \tag{4}$$

where $\mathbf{q}_{i,b}$ denotes the quaternion representing the attitude of the body frame relative to the inertial frame, and $\boldsymbol{\omega}_{i,b}^b$ denotes the angular velocity vector of the body frame relative to the inertial frame referenced in the body frame. The vector $\boldsymbol{\tau}_a^b$ denotes the actuation torques applied to the non-cooperative satellite which in this case will be equal to the aerodynamic torques, $\boldsymbol{\tau}_{aero}^b$, produced by the tugsat, while $\boldsymbol{\tau}_p^b$ denotes perturbing torques which in this work is considered to be zero.

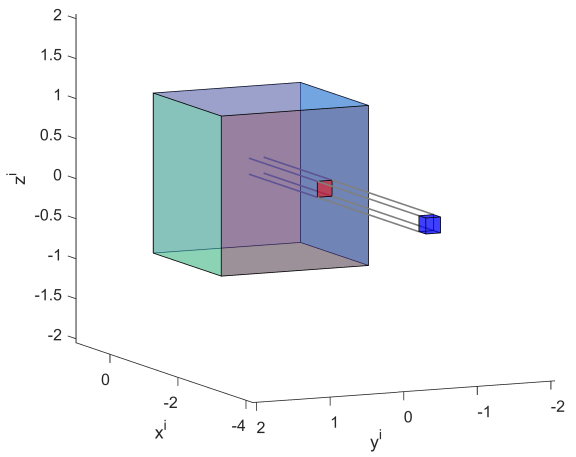

Fig. 1. Illustration of how the tugsat (blue) introduces an aerodynamic wake effect on the non-cooperative satellite (red). As the area of impact is shifted relative to the center of gravity, aerodynamic moments will be generated.

C. Relative Translational Motion

Figure 1 shows the position of the tugsat relative to the non-cooperative satellite and illustrates how the aerodynamic wake affects the non-cooperative satellite. In this work, the tugsat is only allowed to move along the $\mathbf{y}^i$ and $\mathbf{z}^i$ axes to produce different aerodynamic moments. The position of the tugsat can be described as

$$\dot{\mathbf{p}}^i = \mathbf{v}^i \tag{5}$$

$$\dot{\mathbf{v}}^i = \frac{1}{m}\mathbf{f}_a^i \tag{6}$$

where $\mathbf{p}^i$ denotes the position of the tugsat, $\mathbf{v}^i$ its velocity, m its mass, while $\mathbf{f}_a^i$ denotes the actuation force vector that can be created e.g. using translational thrusters. In this work it is set equal to the output from the controllers, i.e. $\mathbf{f}_a^i = \mathbf{f}_d^i$.

D. Modeling the Wake Effect

Seltner et al. have in their work [9] presented a detailed analysis of aerodynamic coefficients for free-flying cubes in hypersonic flows. Figure 2 is an adaption based on [9] to visualize the wake region where the airflow is lower than the surrounding air. As can be observed, there is a wake region directly behind the cube, where the airflow will be lower. Wang et al. show in [10] that the airflow behind a cube can be reduced by more than 30% before it picks up again. It follows that if the tugsat can be positioned correctly relative to the non-cooperating satellite, it is possible to achieve a 30% reduction in airflow, and thereby generating aerodynamic moments that can be used for attitude control.

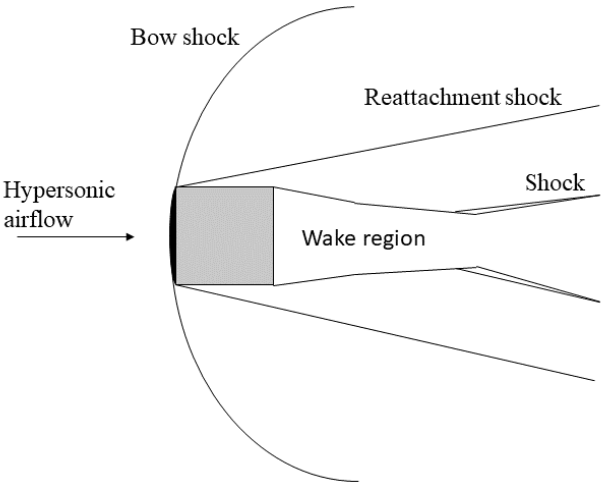

Fig. 2. The wake effect behind a cube flying in hypersonic speeds. Adapted from [9].

III. Calculations of Aerodynamic Moments

Consider again Figure 1 which shows the tugsat relative to the non-cooperative satellite where the impact point of the reduced airflow is shown in red. Assume now that the tugsat is not present. In this case, the airflow hitting the non-cooperative satellite will be uniform and as the non-cooperating satellite is symmetric, no aerodynamic moments will be generated in this case. The aerodynamic drag force acting on the satellite can be found as [11]

$$D = \frac{1}{2}\rho S V_a^2 C_D \tag{7}$$

where ρ is the air density, S is the cross-sectional area, V_a is the airflow, while C_D is the drag coefficient. Force is defined as pressure divided by area, such that this equation can also be interpreted as a sum of small forces that are acting at different sections on the cross-sectional area. From this, it follows that the total drag can be found as

$$D_{total} = D - D_{wake} \tag{8}$$

where D_{wake} denotes the drag force from the wake, which will reduce the overall drag, and can be found as

$$D_{wake} = \frac{1}{2}\rho A V_{wake}^2 C_{D,wake}\,. \tag{9}$$

The parameter A denote the area of the wake, $V_{wake} = (1-\gamma)V_a$ is a reduction in airflow where $\gamma = 0.3$ based on the works by Wang et al. [10], and $C_{D,wake}$ denotes the drag coefficient of the area where the wake hits the non-cooperative satellite. The latter is expected to vary depending on the orientation of the non-cooperative satellite, but is in this work assumed to be constant for simplicity.

TABLE I
Definition of sides on the non-cooperative satellite.

Front	$(\mathbf{p}_1^b, \mathbf{p}_2^b, \mathbf{p}_3^b, \mathbf{p}_4^b)$
Aft:	$(\mathbf{p}_5^b, \mathbf{p}_6^b, \mathbf{p}_7^b, \mathbf{p}_8^b)$
Left:	$(\mathbf{p}_1^b, \mathbf{p}_5^b, \mathbf{p}_7^b, \mathbf{p}_3^b)$
Right:	$(\mathbf{p}_2^b, \mathbf{p}_6^b, \mathbf{p}_8^b, \mathbf{p}_4^b)$
Top:	$(\mathbf{p}_1^b, \mathbf{p}_5^b, \mathbf{p}_6^b, \mathbf{p}_2^b)$
Bottom:	$(\mathbf{p}_3^b, \mathbf{p}_7^b, \mathbf{p}_8^b, \mathbf{p}_4^b)$

Let the radius vector from the center of gravity from the non-cooperative satellite to the impact area be denoted $\mathbf{r}^b$, then the aerodynamic moment can be found as

$$\boldsymbol{\tau}_{aero}^b = \mathbf{S}(\mathbf{r}^b)\begin{bmatrix} -D_{wake} \\ 0 \\ 0 \end{bmatrix}. \tag{10}$$

The aerodynamic moments given in the above equation are related to Figure 1 where the incoming airflow is assumed to move along the positive $\mathbf{x}^i$ axis and the moment can only be created by placing the tugsat in front of the non-cooperative satellite.

A. Non-Cooperative Satellite

The non-cooperative satellite is assumed to be located in the origin of the inertial frame, with eight points denoting its cubic shape. Let the satellite be $2 \times 2 \times 2$ m^3, then its corner points can be found in the body frame as

$$\begin{aligned}
\mathbf{p}_1^b &= \begin{bmatrix} -1 & 1 & 1 \end{bmatrix}^\top \\
\mathbf{p}_2^b &= \begin{bmatrix} -1 & -1 & 1 \end{bmatrix}^\top \\
\mathbf{p}_3^b &= \begin{bmatrix} -1 & 1 & -1 \end{bmatrix}^\top \\
\mathbf{p}_4^b &= \begin{bmatrix} -1 & -1 & -1 \end{bmatrix}^\top \\
\mathbf{p}_5^b &= \begin{bmatrix} 1 & 1 & 1 \end{bmatrix}^\top \\
\mathbf{p}_6^b &= \begin{bmatrix} 1 & -1 & 1 \end{bmatrix}^\top \\
\mathbf{p}_7^b &= \begin{bmatrix} 1 & 1 & -1 \end{bmatrix}^\top \\
\mathbf{p}_8^b &= \begin{bmatrix} 1 & -1 & -1 \end{bmatrix}^\top,
\end{aligned}$$

which can be rotated to the inertial frame as $\mathbf{p}_k^i = \mathbf{R}_b^i \mathbf{p}_k^b$ where $k = 1, .., 8$ and where the rotation matrix can be constructed using the quaternion $\mathbf{q}_{i,b}$. With these corner points, the different sides can be defined as shown in Table I.

B. Tugsat

The tugsat is in this work located at $-10m$ along the $\mathbf{x}^i$ axis and allowed to translate in the $\mathbf{y}^i - \mathbf{z}^i$ plane. The tugsat has a size of $0.2 \times 0.2 \times 0.2$m^3. Further, the orientation of the tugsat is assumed to coincide with the inertial frame, as Seltner et al. show in [9] that the size of the wake can be changed by rotating the tugsat representing another means of controlling the wake effect.

C. Raycasting and Plane Intersection

To determine where the wake hits the non-cooperative satellite, the corners of the tugsat can be projected along the $\mathbf{x}^i$ axis using raycasting (*cf.* [12]), and the impact point of the wake on the satellite surfaces can be calculated using plane intersection. Let the position of one of the tugsat corners be defined as $\mathbf{l}_a$, which can be projected as

$$\mathbf{l}_b = \mathbf{l}_a + \begin{bmatrix} \infty \\ 0 \\ 0 \end{bmatrix} . \tag{11}$$

Depending on the orientation of the non-cooperative satellite there can be two intersection points, one in front, and one in the aft. Let $\mathbf{p}_0$, $\mathbf{p}_1$ and $\mathbf{p}_2$ denote three corners of the satellite, while $\mathbf{l}_a$ and $\mathbf{l}_b$ represent the raycasting line. Then the intersection points can be found as (*cf.* [13])

$$\mathbf{p}_{01} = \mathbf{p}_1 - \mathbf{p}_0 \tag{12}$$

$$\mathbf{p}_{02} = \mathbf{p}_2 - \mathbf{p}_0 \tag{13}$$

$$\mathbf{l}_{ab} = \mathbf{l}_b - \mathbf{l}_a \tag{14}$$

$$t = \frac{(\mathbf{p}_{01} \times \mathbf{p}_{02}) \cdot (\mathbf{l}_a - \mathbf{p}_0)}{-\mathbf{l}_{ab} \cdot (\mathbf{p}_{01} \times \mathbf{p}_{02})} \tag{15}$$

$$u = \frac{(\mathbf{p}_{02} \times -\mathbf{l}_{ab}) \cdot (\mathbf{l}_a - \mathbf{p}_0)}{-\mathbf{l}_{ab} \cdot (\mathbf{p}_{01} \times \mathbf{p}_{02})} \tag{16}$$

$$v = \frac{(-\mathbf{l}_{ab} \times \mathbf{p}_{01}) \cdot (\mathbf{l}_a - \mathbf{p}_0)}{-\mathbf{l}_{ab} \cdot (\mathbf{p}_{01} \times \mathbf{p}_{02})} \tag{17}$$

Then as long as $0 \leq t \leq 1$, $0 \leq u \leq 1$, $0 \leq v \leq 1$ and $u + v \leq 1$ the intersection point between the plane and the raycasting line can be found as

$$\mathbf{l}^i = \mathbf{l}_a + \mathbf{l}_{ab} t \, . \tag{18}$$

D. Putting it Together

Using raycasting together with intersections between the lines and the surfaces, allow the four points representing points of impact of the wake effect on the non-cooperative satellite to be found. Then by comparing the sides, and finding closest points relative to the tugsat, we may calculate of the impact surface area, A. Accounting for edges and corners relative to the tugsat allows one or more individual surfaces to be determined, where the center is found as the average of the points which then define the radius vector $\mathbf{r}^b$ from the center of gravity to the point of impact. Finally, application of (10) allows for attitude control. Figure 3 shows the calculation of the impact on a single surface, Figure 4 shows the impact calculated on an edge, while Figure 5 shows the determination of the impact on a corner.

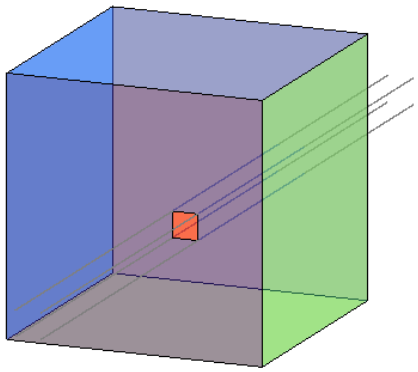

Fig. 3. Impact area on one surface.

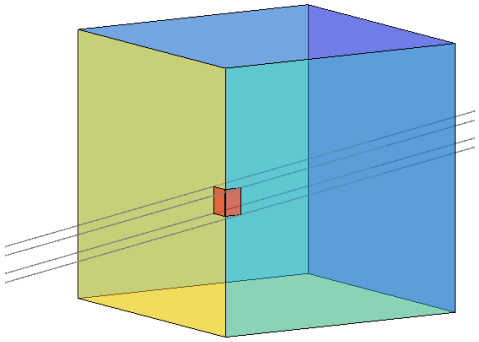

Fig. 4. Impact area on an edge.

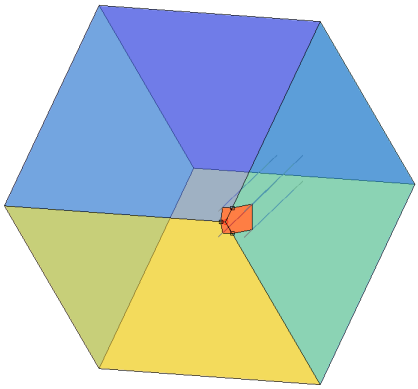

Fig. 5. Impact area on a corner.

IV. Controller Design

In the following, it is assumed that measurements or estimates of the angular velocity and attitude of the non-cooperative satellite are available, e.g. based on computer vision or other sensor systems. Assuming that the tugsat has an initial position inside the area of the non-cooperative satellite, a simple rate controller to stabilize the non-cooperating

TABLE II
PARAMETERS AND VALUES USED FOR THE SIMULATION.

Parameter	Value	Unit
$C_{D,wake}$	1.0	
k_p	1	
k_d	3	
k_q	1	
k_r	1	
ζ	0.8	m
$\mathbf{J}$	$\mathbf{I}$	kgm^2
m	1	kg
$Altitude$	400	km
ρ	$2.803 \cdot 10^{-12}$	kg/m^3
μ	$6.669 \cdot 10^{-11}$	m^3/(kgs^2)
M_{Earth}	$5.9742 \cdot 10^{24}$	kg

satellite can be proposed as follows. Let a desired position be defined as

$$\mathbf{p}_d^i = \begin{bmatrix} x_d & \sigma(-k_r r, -\zeta, \zeta) & \sigma(-k_q q, -\zeta, \zeta) \end{bmatrix}^\top \tag{19}$$

where $k_q, k_r > 0$ are two gains, x_d is a desired point along the $\mathbf{x}^i$ axis, $\boldsymbol{\omega}_{i,b}^b = \begin{bmatrix} p & q & r \end{bmatrix}^\top$, ζ is a parameter that defines how far away from the center of gravity the tugsat is allowed to move, while the saturation function $\sigma(\cdot)$ is defined as

$$\sigma(x, x_{min}, x_{max}) = \begin{cases} x_{min} & \text{if } x < x_{min} \\ x & \text{if } x_{min} \leq x \leq x_{max} \\ x_{max} & \text{if } x > x_{max}. \end{cases} \tag{20}$$

Then a force controller can be proposed as

$$\mathbf{f}_d^i = -k_p(\mathbf{p}^i - \mathbf{p}_d^i) - k_d \mathbf{v}^i \tag{21}$$

where $\mathbf{f}_d^i$ denotes the desired force vector to be applied, while $k_p, k_d > 0$ are proportional and derivative gains. Essentially, the controller allows the tugsat to change its position depending on the angular speed of a given axis and once the non-cooperative satellite has stopped spinning, the tugsat will be located at a position that coincides with the center of gravity, but with a fixed distance, x_d, along the $\mathbf{x}^i$ axis.

V. SIMULATIONS

Table II shows the parameters used for the simulations. Consider a circular trajectory of 400 km where the air density is $2.803 \cdot 10^{-12}$kg/m^3 [14], then the speed of the airflow (or satellite) can be calculated as

$$V_a = \sqrt{\frac{\mu}{r}} \tag{22}$$

where $\mu = M_{Earth} G$ with M_{Earth} as the mass of the Earth and G as the gravitational constant, both given in Table II. The radius can be found as $r = 6778$ km giving $V_a = 7666$ m/s.

Now let the tugsat have an initial position $\mathbf{p}^i(0) = \begin{bmatrix} x_d & 0 & 0 \end{bmatrix}^\top$ with $x_d = -10$, while the non-cooperative satellite has an initial attitude of $\mathbf{q}_{i,b}(0) = \begin{bmatrix} 1 & 0 & 0 & 0 \end{bmatrix}^\top$, an initial angular velocity of $\boldsymbol{\omega}_{i,b}^b(0) = \begin{bmatrix} 0 & 0 & 0.3 \end{bmatrix}^\top$ and its initial position at the origin. Figure 6 shows the angular velocity of the non-cooperative satellite as the tugsat uses the aerodynamic wake effect to stabilize the attitude of the satellite, and as can be observed, the angular velocity goes exponentially to zero. As the aerodynamic wake effect is relative weak, the complete operation takes about 35 days for this maneuver to achieve a close to constant attitude as shown in Figure 7.

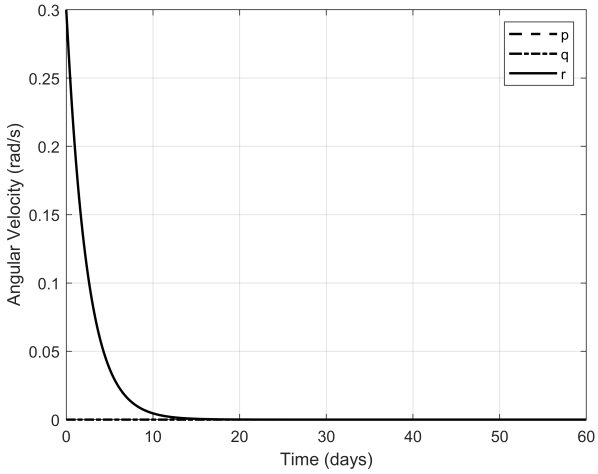

Fig. 6. Angular velocity of the non-cooperating satellite during the operation.

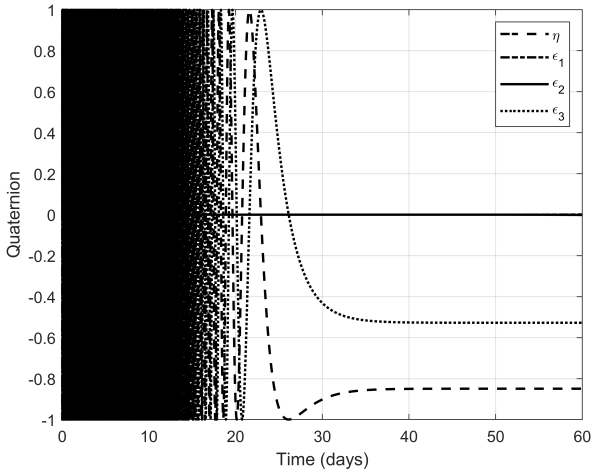

Fig. 7. Quaternion during the operation.

The tugsat uses its position to stabilize the non-cooperative satellite. It starts with $y = 0$, coinciding with the center of gravity, and then moves out to $y = \zeta = 0.8$m before moving back towards the center of gravity as the angular velocity goes to zero. The complete translational motion is shown in Figure 8 where the y position goes to zero as satellite stops spinning.

VI. DISCUSSION

As can be observed through the simulations, it is indeed possible to control a non-cooperative satellite using inter-satellite atmospheric drag, although it takes a long time as the forces and moments are so small. This means that this solution will mainly be applicable to very low Earth orbits

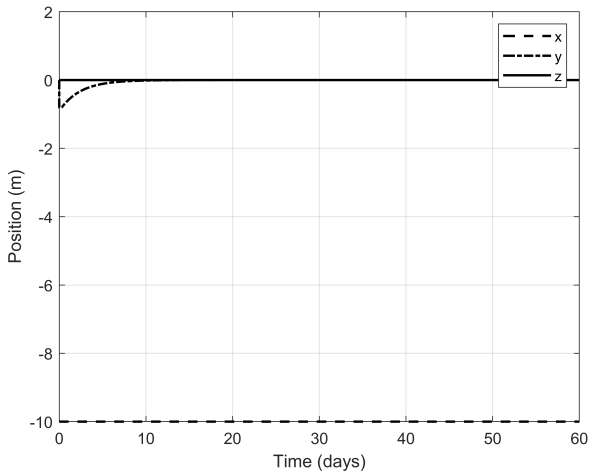

Fig. 8. Tugsat position during operation where the y component converges to zero as the angular velocity goes to zero. The x-component is constantly as -10m.

unless there are other ways of reducing the airflow in the wake. Larger surface area of the tugsat or multiple tugsats represent other ways of increasing the aerodynamic moments to reduce the required time for stabilization.

While this work has only considered the attitude control problem in two axes, a future direction with this work is to extend it to 3D, and also account for the orbital mechanics. Specifically, to build on the work by [15] to account for both relative position and attitude between the satellites. Specifically, relative attitude and position controllers will be active to maintain constant relative distance as the moments introduces translational motions. Another effect that has been ignored in this work is aerodynamic lift, which will occur whenever the satellite has an angle of attack relative to the incoming airflow while being exposed to the tugsat as it removes the symmetry property, and is considered future work.

VII. Conclusion

This paper has presented preliminary results on a novel approach for controlling non-cooperative satellites using inter-satellite atmospheric drag. This can open up new solutions to revitalize inoperative satellites and thereby extending their lifetimes.

Acknowledgement

This work was partially funded by the Norwegian research council through the project 335832 QBDebris: A CubeSat formation for space debris characterization. more info on the project can be found at https://uit.no/project/qbdebris.

References

[1] T. Narumi, N. Uyama, and S. Kimura, "Multipoint-contact attitude control of non-cooperative spacecraft with parameter estimation," in *Proceedings of the IEEE/RSJ International Conference on Intelligent Robots and Systems*, (Hamburg, Germany), 2015.

[2] M. Zhong, Y. Wang, Y. Yang, Z. Wang, L. Tang, and S. Ackland, "Reinforcement learning-based satellite attitude stabilization method for non-cooperative target capturing," *Sensors*, vol. 18, no. 12, pp. 284–289, 2016.

[3] F. Aghili, "Optimal trajectories and robot control for detumbling a non-cooperative satellite," *Journal of Guidance, Control, and Dynamics*, vol. 43, no. 5, 2020.

[4] X. Liu, G. Cai, and W. Chen, "Contact control for grasping a non-cooperative satellite by a space robot," *Multibody System Dynamics*, vol. 50, pp. 119–141, 2020.

[5] J. M. Esposito, "Distributed grasp synthesis for swarm manipulation with applications to autonomous tugboats," in *Proceedings of the IEEE International Conference on Robotics and Automation*, (Pasadena, CA), 2008.

[6] V. P. Bui, H. Kawai, Y. B. Kim, and K. S. Lee, "A ship berthing system design with four tugboats," *Journal of Mechanical Science and Technology*, vol. 25, no. 5, pp. 1257–1264, 2011.

[7] E. Oland, "A command-filtered backstepping approach to autonomous inspections using a quadrotor," in *Proceedings of the 24th Mediterranean Conference on Control and Automation*, (Athens, Greece), 2016.

[8] M. J. Sidi, *Spacecraft Dynamics & Control*. Cambridge University Press, 1997.

[9] P. M. Seltner, S. Willems, and A. Gülhan, "Aerodynamic coefficients of free-flying cubes in hypersonic flowfield," *Journal of Spacecraft and Rockets*, vol. 56, no. 6, pp. 1725–1734, 2019.

[10] Y. Wang, D. Thompson, and Z. Hu, "Numerical investigations on the flow over cuboids with different aspect ratiosand the emitted noise," *Physics of Fluids*, vol. 32, no. 2, 2020.

[11] S. F. Hoerner, *Fluid-Dynamic Drag*. P.O. Box 21992, Bakersfield, CA 93390: Published by the Author, 1st ed., 1965.

[12] S. D. Roth, "Ray casting for modeling solids," *Computer Graphics and Image Processing*, vol. 18, no. 2, pp. 109–144, 1982.

[13] D. Varberg and E. J. Purcell, *Calculus with analytical geometry*. Englewood Cliffs, NJ: Prentice-Hall, Inc., 6th ed., 1992.

[14] NASA, "U.S. standard atmosphere," tech. rep., National Aeronautics and Space Administration, 1976.

[15] R. Kristiansen, *Dynamic synchronization of spacecraft*. PhD thesis, Norwegian University of Science and Technology, Trondheim, Norway, 2008.